Received: 5 July 2021 | Revised: 20 August 2021 | Accepted: 7 September 2021

DOI: 10.1002/wcms.1579

FOCUS ARTICLE

WIREs COMPUTATIONAL MOLECULAR SCIENCE WILEY

A unified molecular-wide and electron density based concept of chemical bonding

Ignacy Cukrowski

Department of Chemistry, Faculty of Natural and Agricultural Sciences, University of Pretoria, Pretoria, South Africa

Correspondence
Ignacy Cukrowski, Department of Chemistry, Faculty of Natural and Agricultural Sciences, University of Pretoria, Lynnwood Road, Hatfield, Pretoria 0002, South Africa.
Email: ignacy.cukrowski@up.ac.za

Edited by: Peter R. Schreiner, Editor-in-Chief

Abstract

Chemical bonding is at heart but, not being a quantum mechanical-defined physical property of a system, is a subject of endless and often fruitless debates. Having so many and very different models of chemical bonding without knowing what this really is does not make it easier. There is, however, a general agreement that concentrating electron density (ED) in and delocalizing ED to internuclear region is always associated with minimizing system's energy and synonymous with chemical bonding. Fragment, atomic, localized, delocalized, and interatomic (FALDI)-based density analysis involves entire space occupied by a molecule. From this molecular-wide and density-based methodology, it is possible to quantify localized and delocalized by all atoms ED at any coordinate **r**, including critical points on Bader's molecular graphs. Each atom and atom-pair contributions of delocalized density are quantified to reveal major players in the all-atom and molecular-wide chemical bonding. Partitioning the total ED to individual molecular or natural orbital's contributions using MO-ED and MO-DI methods, in conjunction with one dimensional (1D) cross section methodology, generates an orbital-based molecular-wide picture. This provides, besides reproducing results from FALDI, qualitative description of orbitals' nature that correlates well with classical understanding of bonding, nonbonding, and antibonding orbitals. A qualitative and quantitative impact of an immediate, distant, or molecular-wide molecular environment on intra- and intermolecular di-atomic, intra- and interfragment interactions is the domain of the Fragment Attributed Molecular System Energy Change (FAMSEC) family of methods. The FALDI, FAMSEC, MO-ED, MO-DI, and 1D cross section methodologies provide consistent and quantifiable physics-based picture of molecular-wide chemical bonding without invoking unicorns, such as a chemical bond.

This article is categorized under:

Electronic Structure Theory > Density Functional Theory
Electronic Structure Theory > Ab Initio Electronic Structure Methods
Molecular and Statistical Mechanics > Molecular Interactions

KEYWORDS
chemical bonding, density topology, DFT, FALDI, FAMSEC

1 | INTRODUCTION

Chemical bonds and bonding are at heart of all chemists and, not surprisingly, the number of books dedicated to bonds/bonding[1–7] is steadily growing. The number of different chemical bonds proposed by chemists is large (covalent, polar-covalent, ionic, hydrogen, resonance assisted H-bonds, dihydrogen, hydrogen–hydrogen, halogen, lithium, dative, coordination, σ-hole, homopolar and heteropolar, and many more) and continuously growing.

Notably, neither atom nor chemical bonds are directly defined in the quantum mechanical (QM) description of molecular systems. This means that any attempt to define the two fundamental terms in understanding and development of chemistry must introduce some degree of arbitrariness. Chemical bonds and bonding can be seen as terms at the borderline of two worlds, that of chemistry and physics. As nicely put by Frenking and Krapp,[8] chemists developed many unicorns with hope to "bring law and order, health and good fortune, fame and satisfaction to chemists who would otherwise be lost in a pandemonium of experimental observations." However, fundamental understanding of physics-defined mechanism(s) leading to "chemical" bonding and chemical bond formation (as perceived by classical chemists) needs an accurate QM treatment of entire molecular system.

Clearly, the phenomenon called chemical bonding between (among?) atoms of a molecular system made of many nuclei and "plenty" of electrons are extremely difficult to define, describe, and quantify. Understanding and describing bonding might be seen as nearly an impossible task because, according to Hirshfeld[9] "It should be superfluous to emphasize that, as there are no actual atoms in a molecule, any definition of atomic fragments must be essentially arbitrary." Hence, there are also different models of atoms in molecules. For instance, in the world of mathematical objects called orbitals, an atom is seen as a positively charged nucleus with electron-carrying atomic orbitals cantered on it. A protocol involving operations on spherically averaged ground-state atomic densities as well as the promolecule and actual molecular densities, proposed by Hirshfeld,[9] is seen as a first example of "fuzzy atoms" in molecules.[10] Bader's definition of an atom[11] is different as it is based on mathematically exploring the properties of the molecular electron density (ED), a physical observable and measurable descriptor in the three dimensional (3D) internuclear space.[12,13] In Bader's world, atoms have well-defined shapes but seldom perfectly spherical and, surprisingly to orthodox chemist, the size and shape of an atom varies in larger molecular environments. Moreover, Bader's description of chemical bonding was drastically different to that of orbital-based concepts (an overlap of atomic orbitals or constructive interference of molecular orbitals [MOs]) or Lewis definition (electron pair sharing). He has introduced a concept of chemical bonding as an ED bridge (named a bond path [BP]) linking atoms of a molecular system and made it clear that a BP is not a chemical bond but BP linking two atoms reveals bonded atoms in a molecular system.[14] In addition, an associated with each BP a unique point named a bond critical point (BCP) proved to be very useful. Notably, the density at a BCP is most reproducible experimentally[12] and numerous properties computed at BCPs were used in describing many modes and kinds of bonding in different molecular environments.

However, the honeymoon of Bader's theory of bonding came to a 'standstill' when Matta et al[15] claimed that the homopolar CH--HC contact in planar biphenyl, phenanthrene, and other compounds "rather than denoting the presence of 'nonbonded steric repulsions,' makes a stabilizing contribution of up to 10 kcal mol^{-1} to the energy of the molecule in which it occurs."

Instantly, the chemists' fraternity found itself in two and opposing each other camps. Namely, the quantum chemical topology methods (QTAIM [Quantum Theory of Atoms in Molecules],[11] IQA [Interacting Quantum Atoms],[16,17] FOHI [Fractional Occupation Hirshfeld-I][18] and FAMSEC [Fragment Attributed Molecular System Energy Change][19]) and the wavefunction-based camp (MO,[1,2] VB [valence bond][1,2] theory, NBO [natural bond orbital],[6] etc.). The latter camp is strongly opposing Bader's interpretation:

1. "In conclusion, the presented results indicate that there is no need to rewrite chemical textbooks. The existence of a BCP is neither a necessary nor a sufficient condition for a sensible definition of a chemical bond." "Our results are in complete agreement with the traditional view of this H—H interaction as steric (Pauli) repulsion." "... we suggest to abandon the use of the term "hydrogen–hydrogen bonding" in cases ... ."[20]

2. "...the concept of energetically unfavorable nonbonded H--H interactions at short H--H separations has been very productive in explaining organic stereochemistry, and so the idea that such interactions are energetically favorable would, if correct, overturn much chemical thinking built up over many decades."[21]

Even though the two camps successfully used QM in describing chemical bonding for decades, they appear to drift apart even further with the growing number of unusual di-atomic interactions linked with a BP.

In sections that follow, an attempt will be made to convince the reader that both, orbital and density approaches, can and indeed do provide complementary description of molecular system. To achieve a harmony, however, it is strongly advocated that an old-fashioned and outdated unicorn of ill-defined chemical bond(ing) should be replaced by rigorous and physics-based description of molecular-wide all-atom density contributions to *any coordinate* ***r*** *in 3D space* occupied by a molecule. This is because "There are only two forces operative in chemistry, the Feynman force exerted on the nuclei and the Ehrenfest force exerted on the electrons"[14] and this applies to any coordinate **r** or part of a molecular system.

2 | RELATIVE MOLECULAR STABILITY AND HIGHLY QUESTIONABLE BPs

Polyamines are extremely flexible molecules and often unexpected BPs are found in equilibrium structures.[22] Molecular graphs of protonated triethylenetetramine (*trien*, HL) of (i) the lowest energy conformer (LEC; HL-1) and (ii) the second lowest energy HL-2 (with $\Delta E = E_{\text{HL-2}} - E_{\text{HL-1}} = 0.70$ kcal/mol) found at the MP2 level are shown in Figure 1.

All classical covalent bonds and intramolecular NH···N H-bonds linking terminal N25 and N28 are perfectly recovered by BPs. However, it is rather difficult to understand why HL-1 is the LEC as some cross-ring BPs would not be easily accepted as representing chemical bonding. Hence, one might ask:

1. Why a BP(N25,N27) is formed at all and is seen only in the lowest energy conformer? Clearly, atoms of this homopolar bonding must be involved in highly repulsive and destabilizing the molecule interaction.
2. Why CH···HC BPs are formed at all and more BP(H,H) were found in lowest energy conformers?[22]
3. Are the BPs linking N,N and H,H atom-pairs privileged exchange-correlation channels[23] or just a topological artifact?
4. Would the energy of HL-1 be even lower if not for the N--N and CH--HC clashes? Can one explore it without artificial partitioning of a molecule?

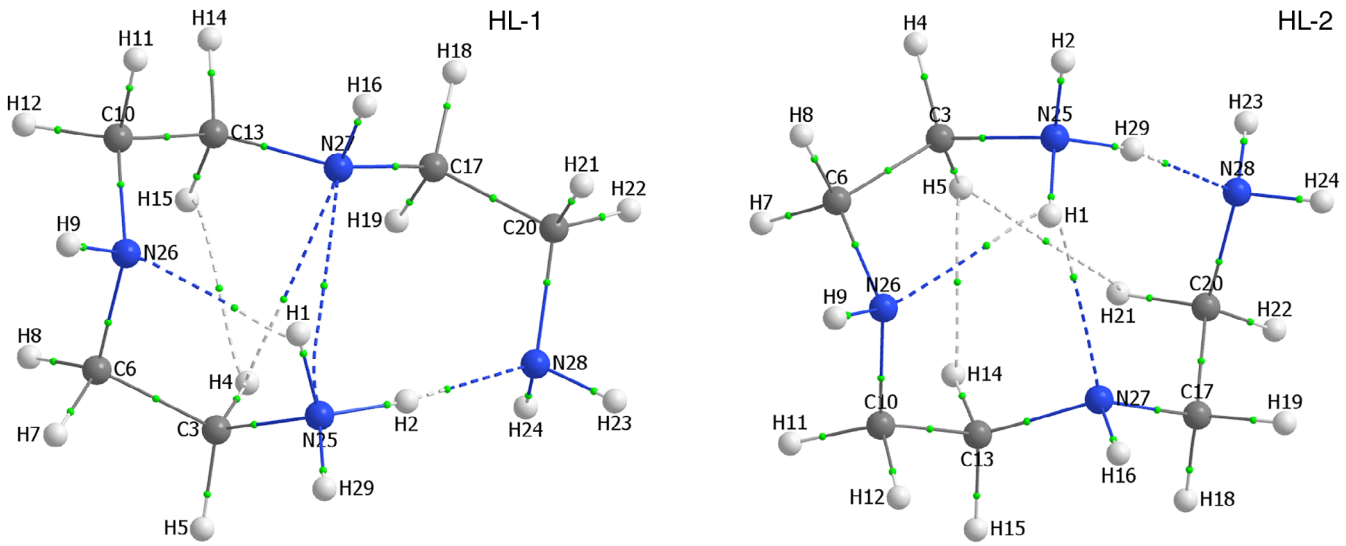

FIGURE 1 Molecular graphs (at the MP2/6-311++G(d,p)/PCM level in water) of the lowest HL-1 and higher HL-2 (by 0.7 kcal/mol) energy conformers of triethylenetetramine L protonated on the terminal N25. Adapted from Reference 22

5. Do NH···N classical H-bonds compensate over the energetic "damage" done by the clashing N,N and H,H atom-pairs?
6. What is the energy contribution made to a molecule by classical, IUPAC-defined[24,25] H-bonds and steric contacts?
7. Considering HL-1, why a BP between N27 and H4 forms a CH···N H-bond with d(N,H) = 2.60 Å but is not observed between N27 and H1 with d(N,H) = 2.48 Å? This would result in a stronger N25H1···N27 interaction and most importantly remove a controversial BP between N27 and N25.
8. Why C13H14--H21C20 contact in HL-2 is not privileged relative to the BP-linked C3H5···H21C20 interaction even though (i) d(H14,H21) of 2.30 Å is much shorter than d(H5,H21) = 2.47 Å with the latter being larger than the sum of the van der Waals radii.

Due to flexibility of polyamines, an orthodox chemist might argue that these conformers (i) should spontaneously re-arrange in order to eliminate any steric CH--HC or N--N and energy-destabilizing contact and, since this is not the case, (ii) interpreting some of BPs as representing chemical bonds and bonding cannot be correct.

3 | NEW TOOLS IN EXPLORING AND UNDERSTANDING CHEMICAL BONDING

Properties of modified molecules or their fragments were often used as arguments to demonstrate a destabilizing impact made by the steric H--H contact. To this effect:

a. Two different molecules (ligands) were used to argue relative stability of Ca(II) complexes and stability lowering effect due to structurally identified "sterically unfavorable nonbonded H--H two interactions" between three pyridine rings.[21]
b. Molecules were deprotonated to form anions[21] or trimmed from H-atoms.[26]
c. Radicals were formed by cutting molecules to pieces.[26,27]

These are just a few examples of rather extreme approaches that often produced nonphysical and unrealistic states of a molecular systems.[28] It is of paramount importance to realize that each molecule has its own molecular-wide ED-signature that is as unique as a human fingerprint. Even small movement of nuclei, for example, due to the zero-point nuclear vibrations, might change a shape of BPs and internuclear connectivity on a molecular graph.[29] By cutting a molecule to pieces or removing some fragments produces entirely new constellation of nuclei that will spontaneously drive new density arrangement to minimize system's energy. The new density distribution, a new fingerprint of a radical, is not directly comparable with that in a molecule. In addition, one never knows where to place an excess of electrons meaning that "There is no unique choice for the intermediate wave functions"[28] when energy decomposition analysis is performed.

Without a doubt, new tools that preserve molecule's integrity are required to qualitatively and quantitatively explore the existing density distribution throughout a molecule by topology- and MO-based approaches and to quantify energy contributions made by polyatomic fragments to a molecular system.

Bader's molecular graphs will be used for illustration purposes as they recover not only classical 2-atom chemical bonds but also reveal "unusual and unexpected" topological features that will aid in describing applicability and usefulness of the new tools discussed in sections that follow. However, as interpretability of Bader's BP in terms of chemical bonds is not the subject of this review, a density bridge (DB) rather than BP and a critical point (CP) rather than BCP are used to avoid any connotation to chemical bonding. Although "edge," "link," or "line" were suggested,[30] both DB and CP are well-defined features of ED distribution within a molecular system and, notably, the concept of a "bridge of density" was introduced by London already in 1928.[14]

3.1 | 1D cross-sections of the electron and deformation density distributions

The one dimensional (1D) cross-section of ED is generated by plotting ED along the eigenvector, usually corresponding to the λ_2 eigenvalue of the Hessian matrix; for brevity, it is called the λ_2-eigenvector.[31] This simple protocol provides a visual inspection of ED variation for any atom-pair. Typically, one starts from coordinates of the selected (3,–1) CP but

the same protocol is followed starting at any coordinate **r**, for example, from a minimum density point (MDP) identified in the internuclear region where no DB is observed.

The first reported examples of ED 1D cross-sections[31] are shown in Figure 2a. They were obtained for (i) the most common and attractive intermolecular H-bond with a DB in the lowest energy water dimer **d1** (circles in Figure 2a) and (ii) highly repulsive interaction between O-atoms linked by DB in water dimer **d2**—see dashed line in Figure 2a.

Remarkably, even though these two interactions could hardly be more different, both traces, that is, trends in the total density in the vicinity of CP(O1,H5) (it is closer to H5) and CP(O1,O4) (it is exactly in the middle between O-atoms in **d2**) are qualitatively the same even though topological properties at both CPs are very different. Traces in Figure 2a show concentrated density in both cases and, not surprisingly, exactly the same picture immerged from the Noncovalent Interaction (NCI) method[32–34] with blue discs (located at respective CPs) representing $\lambda_2 < 0$. These trends represent a typical static (as is along the λ_2-eigenvector) picture of ED of the intermolecular interaction linked with a DB. However, the processes leading to these two DBs formation, as revealed by the deformation density ($\Delta\rho(\mathbf{r})$), were opposite; $\Delta\rho(\mathbf{r}) > 0$ with an inflow of ED into the bonding region took place only on **d1** formation whereas it was partly removed (*dissipated*) from the bonding region of the O···O interaction.[31]

The O···H, NH···N, CH···HC, CH···HN, NH···HN, CH···N, H···H, O···O, and N···N intra- and intermolecular interactions were studied[31] in: s-*cis* and s-*trans* bipyridine (bpy, L) and its HL and H_2L protonated forms, nitrilotri-3-propionic acid, a polyamine *trien*, and differently arranged four water dimers. Results showed that there is no obvious relationship between the presence (or absence) of a DB and:

a. Highly attractive or repulsive nature of an interaction.
b. Internuclear distance.
c. Inflow or outflow of density to internuclear "bonding" region.
d. Sign of λ_2.

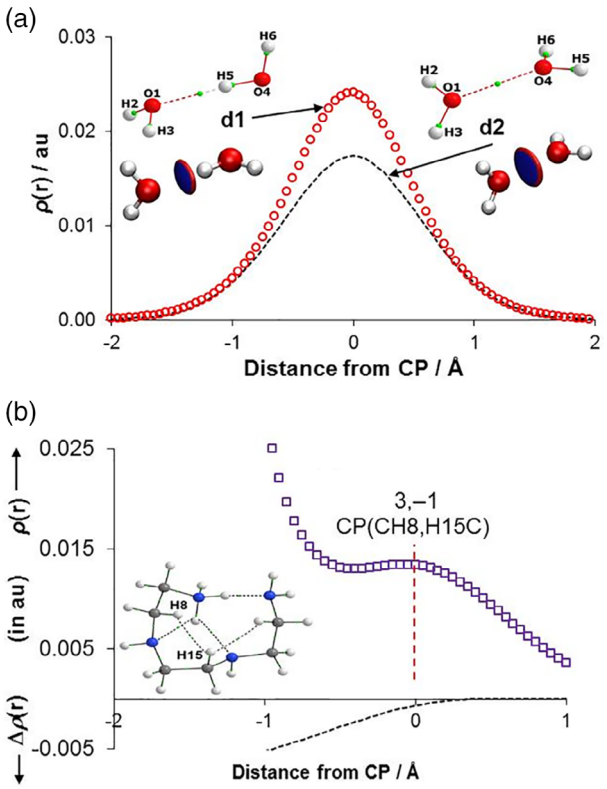

FIGURE 2 (a) Cross-sections of ED along the λ_2–eigenvector originating from CP(O1,H5) in water dimer **d1** and CP(O1,O4) in water dimer **d2**. Molecular graphs of **d1** and **d2** and NCI isosurfaces for both water dimers are also shown. (b) Cross-section of ED (squares) and deformation density (dashed line) along the λ_2–eigenvector originating from CP(H8,H15) in polyamine *trien* shown as an inset. Adapted from Reference 31

Hence, it became abundantly clear that typical topological QTAIM, IQA, NCI indices, even when combined, could not be used to conclusively explain a chemical meaning of a DB.

However and importantly, it showed that the molecular environment has an immense impact on the indices describing a diatomic interaction. For instance, Figure 2b shows CH8···H15C with a DB in the equilibrium structure of a lower energy conformer of *trien*. The H-atoms are involved in the IQA-defined repulsive Coulombic but overall an attractive interaction dominated by the exchange-correlation term, a description equally applicable to a classical covalent C—C bond.[35] However, the process of the DB(H8,H15) formation is opposite to that of a covalent bond or classical DB(O1,H5) of the H-bond in **d1**. Notably, the outflow of density was found (see dashed trace-line for $\Delta\rho(\mathbf{r}) < 0$ in Figure 2b) that is also observed for the destabilizing and highly repulsive O1···O4 interaction in **d2**.[31] These findings strongly suggest that atoms contribute not only to a "bonding" region of a diatomic interaction but also to any point **r** of a 3D space occupied by a molecule.

3.2 | Revealing a holistic multicenter and molecular-wide nature of interactions

3.2.1 | FALDI-based decomposition of ED

If an *n*-center ($n \geq 2$) interaction takes place then it must create its signature in the "bonding" internuclear region of any atom-pair. To explore a multicenter character of an interaction, the fragment, atomic, localized, delocalized, and interatomic (FALDI[36]) ED decomposition scheme has been extended.[37,38] The QTAIM-defined atomic population $N(\mathrm{A})$, that is, the average number of electrons found in the atomic basin of atom A (Ω_A),[11] can be calculated either by integrating the molecular ED over Ω_A, Equation (1)

$$N(\mathrm{A}) = \int_\mathrm{A} \rho(\mathbf{r}) d\mathbf{r} \tag{1}$$

or using $\mathbf{S}^\mathrm{A}$, the atomic overlap matrix (AOM)

$$N(\mathrm{A}) = tr\left(\mathbf{S}^\mathrm{A}\right) \tag{2}$$

for which its elements represent the overlap between all MO pairs over Ω_A and when, for simplicity, a single-determinant and spin-restricted wavefunction is considered, one can write elements as

$$S_{ij}^\mathrm{A} = \sum_{ij} \int_\mathrm{A} \chi_i^*(\mathbf{r}) \chi_j(\mathbf{r}) d\mathbf{r} \tag{3}$$

However, one must realize that, for example, canonical MOs are molecular-wide and delocalized portion of $N(\mathrm{A})$ can be also found elsewhere. Hence, the $g_\mathrm{A}(\mathbf{r})$ function, the central quantity in the Domain Averaged Fermi Hole (DAFH) approach,[39–41] has been incorporated in FALDI, Equation (4)

$$g_\mathrm{A}(\mathbf{r}) = \sum_{ij} \chi_i^*(\mathbf{r}) \chi_j(\mathbf{r}) S_{ji}^\mathrm{A} \tag{4}$$

A convenient feature of the DAFH approach makes it possible to compute, for example, atomic population $N(\mathrm{A})$ by exploring the entire space of a molecule when the $g_\mathrm{A}(\mathbf{r})$ function is integrated, Equation (5)

$$N(\mathrm{A}) = \int_{-\infty}^{\infty} g_\mathrm{A}(\mathbf{r}) d\mathbf{r} \tag{5}$$

To take advantage of DAFH features, localization (*loc*-ED)

$$\mathcal{L}_{\mathrm{A}}(\mathbf{r}) = \sum_{ij} \chi_i^*(\mathbf{r})\chi_j(\mathbf{r})\left(\mathbf{S}^{\mathrm{A}}\mathbf{S}^{\mathrm{A}}\right)_{ji} \tag{6}$$

and delocalization (*deloc*-ED)

$$\mathcal{D}_{\mathrm{A,B}}(\mathbf{r}) = \sum_{ij} \chi_i^*(\mathbf{r})\chi_j(\mathbf{r})\left(\mathbf{S}^{\mathrm{A}}\mathbf{S}^{\mathrm{B}}\right)_{ji} \tag{7}$$

ED *distributions* were defined in FALDI, where $\mathbf{S}^{\mathrm{A}}\mathbf{S}^{\mathrm{A}}$ is the matrix product of $\mathbf{S}^{\mathrm{A}}$ with itself and $\mathbf{S}^{\mathrm{A}}\mathbf{S}^{\mathrm{B}}$ is the sum of matrix products $\mathbf{S}^{\mathrm{A}}\mathbf{S}^{\mathrm{B}} + \mathbf{S}^{\mathrm{B}}\mathbf{S}^{\mathrm{A}}$. Notably, integrating the *deloc*-ED for an atom A over the 3D space occupied by a molecule generates the QTAIM-defined delocalization index *DI*(A,B),

$$\int_{-\infty}^{\infty} \mathcal{D}_{\mathrm{A,B}}(\mathbf{r})d\mathbf{r} = tr\left(\mathbf{S}^{\mathrm{A}}\mathbf{S}^{\mathrm{B}}\right) = \delta_{\mathrm{QTAIM}}(\mathrm{A,B}) = DI(\mathrm{A,B}) \tag{8}$$

and very much the same applies to integrating $\mathcal{L}_{\mathrm{A}}(\mathbf{r})$ that produces the QTAIM-defined localization index.[37,38] In such a way the real-space distributions of orthodox localization and delocalization indices were achieved. Furthermore, FALDI-defined *loc*-ED and *deloc*-ED distributions are used to decompose $g_{\mathrm{A}}(\mathbf{r})$ and the total density at any coordinate **r,**

$$g_{\mathrm{A}}(\mathbf{r}) = \mathcal{L}_{\mathrm{A}}(\mathbf{r}) + \sum_{\mathrm{B}\neq\mathrm{A}} \frac{1}{2}\mathcal{D}_{\mathrm{A,B}}(\mathbf{r}) \tag{9}$$

$$\rho(\mathbf{r}) = \sum_{\mathrm{A}} g_{\mathrm{A}}(\mathbf{r}) = \sum_{\mathrm{A}} \mathcal{L}_{\mathrm{A}}(\mathbf{r}) + \sum_{\mathrm{AB}} \mathcal{D}_{\mathrm{A,B}}(\mathbf{r}) \tag{10}$$

To explore multicenter nature of bonding, the main focus is on the origin of delocalized ED contributing to the total electron density (*tot*-ED) at any coordinate **r** in real-space.[37] FALDI-based analysis showed that an atom-pair can contribute *deloc*-ED along the λ_2-eigenvector originating either from a CP on a DB(A,B) or a MDP(A,B), in a *concentrating*, *depleting* or *reducing* fashion. When nomenclature adopted in MO bonding theory is used, these three modes can be seen, respectively, as of: (1) *bonding* ($\mathcal{D}_{\mathrm{A,B}}(\mathbf{r}) > 0$ and $\partial\mathcal{D}^2_{A,B}/\partial^2\mathbf{r} < 0$), (2) *nonbonding* ($\mathcal{D}_{\mathrm{A,B}}(\mathbf{r}) > 0$ and $\partial\mathcal{D}^2_{A,B}/\partial^2\mathbf{r} > 0$), or (3) *antibonding* ($\mathcal{D}_{\mathrm{A,B}}(\mathbf{r}) < 0$) nature. Importantly, a specific *deloc*-ED $\mathcal{D}_{\mathrm{A,B}}(\mathbf{r})$ distribution might contribute differently to individual internuclear regions. Hence, it can concentrate *deloc*-ED between atomic basins Ω_{A} and Ω_{B} but deplete in the $\Omega_{\mathrm{B}}|\Omega_{\mathrm{C}}$ interatomic region.

Characteristic trends of the three contributions along the λ_2-eigenvector originating from (3, –1) CP(H6,N11) of the classical intramolecular hydrogen bond in the LEC of β-alanine[37] are shown in Figure 3a. The total bonding (constructive or concentrating) contribution (the blue trace-line in Figure 3a) originates mainly from the O5,H6, H6,N11, N11,H12, and N11,H13 atom-pairs with 33.4, 26.9, 6.2, and 5.2%-fraction contributions amounting to 87% of the total "bonding" *deloc*-ED that constitutes 71.7% of the total *deloc*-ED. The molecular region from which the *deloc*-ED of the bonding nature mainly came from is shown as 3D-isosurface in Figure 3a whereas main "bonding" *deloc*-ED contributions are presented in Figure 3b where the combined contribution made by N11,H12, and N11,H13 atom-pairs is shown as N11–{H12,H13} fragment.

It is seen in Figure 3b that this is not the atoms directly involved in the intramolecular H-bonding (H6 and N11) that delocalized most density of bonding nature to the CP of a DB(H6,N11); the O5,H6 atom-pair contributed 41% that is 8% more than the H6,N11 atom-pair. Moreover, significant bonding *deloc*-ED contributions of 2.0, 2.0, and 0.9% were made by distant H10,N11, C2,N11, and O5,O7 atom-pairs, respectively. The main contribution of 99% to *nonbonding* *deloc*-ED came from the C8,N11 atom-pair whereas the O5,N11 atom-pair contributed most (72%) to *antibonding* ED at the CP(H6,N11). The FALDI-based analysis has shown that the DB(H6,N11) is a product of (i) a cooperative ED delocalization made by most atoms of the molecule and (ii) competing (*bonding*, *non*-, and *antibonding*) contributions made by numerous atom-pairs.[37]

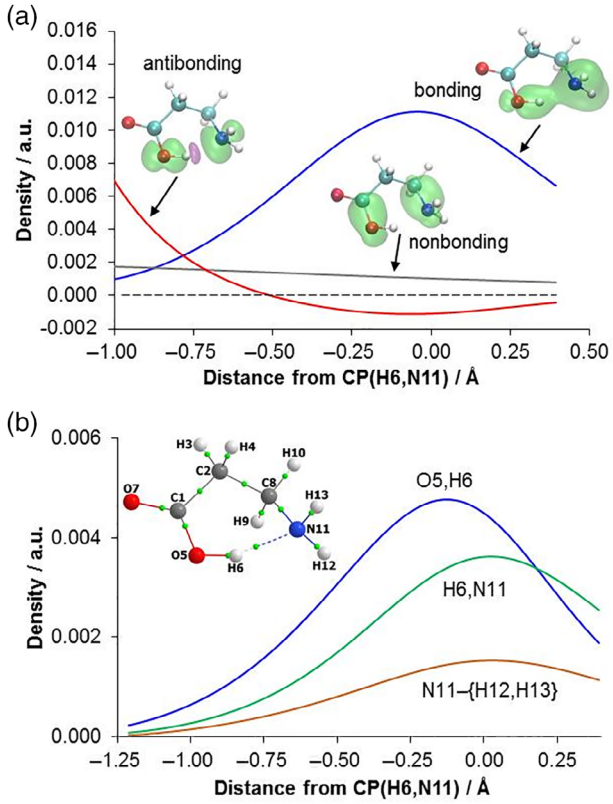

FIGURE 3 (a) FALDI-based decomposition of the *deloc*–ED into constructive (i.e., concentrating = bonding nature; blue trace), nonconstructive (i.e., depleting = nonbonding nature; gray trace) and deconstructive (i.e., removing = antibonding; red trace) electron correlation at the CP(H6,N11). Relevant isosurfaces of the major bonding (combined O5,H6 + H6,N11 + N11–{H12,H13}), nonbonding (C1, O5 +C8,N11) and antibonding (O5,N11) contributions at the CP(H6,N11) are also shown. Color coding: green, positive; purple, negative. (b) FALDI-based decomposition of the *deloc*-ED of bonding nature. Major contributing atom-pairs as well as molecular graph of β-alanine are shown. Adapted from Reference 37

3.2.2 | Molecular-wide charge redistribution on a conformational change

Figure 4 shows throughout-a-molecule charge redistributions taking place on a structural change from a linear conformer of β-alanine to the LEC (Figure 4a) and higher (by 5.9 kcal/mol) energy conformer (HEC, Figure 4b).[42] A proper red-shifted and improper blue-shifted intramolecular H-bonds are present in LEC and HEC, respectively. All atoms, hence also functional groups of the molecule experienced, relative to the linear conformer, significant changes in net atomic charges but patterns are drastically different in both conformers. An inflow of density (+38*me*) to the COOH functional group of the LEC (Figure 4a) and outflow of density (−5*me*) from the NH_2 functional group of the HEC (Figure 4b) took place; both functional groups contain H-atom involved in the intramolecular H-bonding. The largest inflow (+38*me*) and outflow (−60*me*) in the LEC is observed, respectively, for the COOH and NH_2 functional groups, whereas largest changes of +27*me* and −22*me* are seen for two middle CH_2 groups of the HEC.

3.2.3 | FAMSEC-based impact of molecular environment on an interaction

The impact of a molecular environment on the two different H-bonds, was also investigated by the FAMSEC method.[19] Originally, FAMSEC was designed to investigate classical NCIs and to quantify their impact on molecular stability without cutting a molecule into nonphysical pieces, that is, all classical or "structural" covalent bonds are preserved. Notably, FAMSEC quantifies energetic changes from the reference (*ref*) to final (*fin*) state, for example, structural rearrangement that results in a new intramolecular H-bond formation. Considering an *n*-atom molecular fragment $\mathcal{G}$

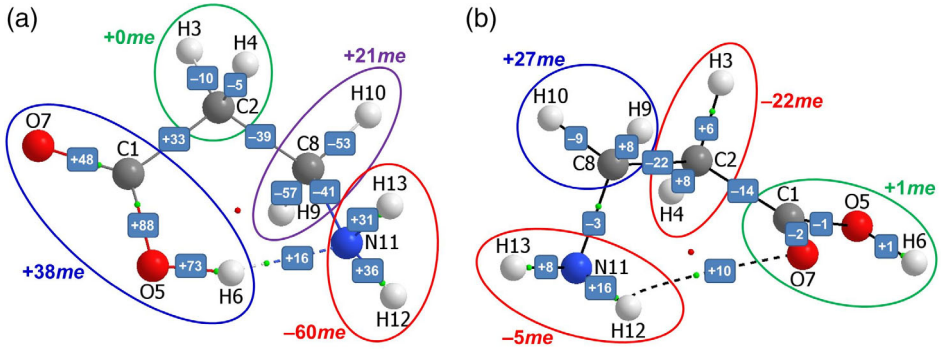

FIGURE 4 Molecular graphs of the lowest (a) and higher (b) energy conformers of β-alanine with intramolecular "proper red-shifted" OH···N and "improper blue-shifted" NH···O H-bonds, respectively. Values at the ovals encompassing functional groups show changes in a sum of net atomic charges and values placed on DBs show $\Delta Q = Q(\mathrm{A}) - Q(\mathrm{B})$, both in *me*. A linear conformer of β-alanine was used as a reference state. Positive values indicate either an inflow of electrons (for net atomic charges) or an increase in charge polarization ΔQ between two atoms. Data obtained at the MP2/aug-cc-pvDZ level. Adapted from Reference 42

(e.g., a 4-atom X—H···Y—Z fragment representing an IUPAC notation for a H-bond[24,25]) one can compute its energy change on *ref* → *fin* as

$$loc - \mathrm{FAMSEC} = \Delta E^{\mathcal{G}}_{\mathrm{self}} + \Delta E^{\mathcal{G}}_{\mathrm{int}} \tag{11}$$

where $\Delta E^{\mathcal{G}}_{\mathrm{self}}$ accounts for the change in the self-atomic energies of all atoms of $\mathcal{G}$, Equation (12)

$$\Delta E^{\mathcal{G}}_{\mathrm{self}} = {}^{fin}\sum_{\mathrm{A}\in\mathcal{G}} E^{\mathrm{A}}_{\mathrm{self}} - {}^{ref}\sum_{\mathrm{A}\in\mathcal{G}} E^{\mathrm{A}}_{\mathrm{self}} \tag{12}$$

and $\Delta E^{\mathcal{G}}_{\mathrm{int}}$ stands for the intrafragment interaction energy change, Equation (13)

$$\Delta E^{\mathcal{G}}_{\mathrm{int}} = {}^{fin}\sum_{\substack{\mathrm{A,B}\in\mathcal{G}\\ \mathrm{A}\neq\mathrm{B}}} E^{\mathrm{A,B}}_{\mathrm{int}} - {}^{ref}\sum_{\substack{\mathrm{A,B}\in\mathcal{G}\\ \mathrm{A}\neq\mathrm{B}}} E^{\mathrm{A,B}}_{\mathrm{int}}. \tag{13}$$

If energy localized to a selected fragment $\mathcal{G}$ decreases (*loc*-FAMSEC <0) then it means that the selected fragment became stabilized in *fin*. This fragment contribution to molecular energy on *ref* → *fin* can be obtained from.

$$mol - \mathrm{FAMSEC} = loc - \mathrm{FAMSEC} + \Delta\sum_{\mathrm{X}\in\mathcal{H}} E^{\mathcal{G}\mathrm{X}}_{\mathrm{int}} \tag{14}$$

where the last term accounts for interaction energy changes between atoms of the selected fragment $\mathcal{G}$ and all remaining atoms of a molecule that constitute a molecular fragment $\mathcal{H}$. When *mol*-FAMSEC <0 then $\mathcal{G}$ stabilized a molecule on a *ref* → *fin* structural change and this could be due to either (i) dominant and of stabilizing nature contribution coming from *loc*-FAMSEC, (ii) favorable change in molecular environment experienced by the fragment $\mathcal{G}$ when in *fin* due to dominant attractive interactions with the atoms of $\mathcal{H}$, or (iii) both energy terms in Equation (14) changed favorably.

Using a *mol*-FAMSEC energy term, the H···Y, X—H···Y, X—H···Y—Z (IUPAC notation), and W—X—H···Y molecular fragments' energy contributions to β-alanine on *ref* → *fin* were quantified. Results showed that the *mol*-FAMSEC values largely depend on interactions between a selected fragment and the remainder of a molecule; they varied between +125 and −85 kcal/mol in LEC and +50 and −31 kcal/mol in HEC. Consequently, the W—X—H···Y and X—H···Y

fragments stabilized both, LEC and HEC, conformers whereas the IUPAC-defined intramolecular H-bond (the X—H···Y—Z fragment) destabilized HEC.

To conclude, increased or decreased stability of a molecular system on the formation of an intramolecular interaction cannot be seen as a local event but rather inclusive of the entire molecule. This has also been nicely recovered from FALDI-based analysis.[42] It showed that due to specific atomic deformation density (DD) contributions at CPs of intramolecular interactions in LEC and HEC, the total-DD *increases* only at CP(H6,N11) and its vicinity in LEC, even though a DB is observed in both conformers.

3.3 | Quantifying and characterizing orbitals' contributions to a density topology

3.3.1 | Insight from the MO-ED method

It is generally recognized that "the shapes of MOs do not easily lend themselves to meaningful chemical interpretation"[21] and this is particularly true in larger molecules.[35] A protocol named MO-ED has been developed[43] to quantify and characterize molecular canonical and natural individual orbitals' contributions to ED at any coordinate **r**. The protocol involves a combination of (a) 1D cross-sections of the ED described in Section 3.1, (b) decomposition of the total electron density at a specifically selected coordinate **r** into contributions made by each orbital using Equation (15),

$$\rho(\mathbf{r}) = \sum_{i}^{N_{MO}} \nu_i |\chi_i(\mathbf{r})|^2 \tag{15}$$

where χ_i is an MO with occupation ν_i, and (c) computing the partial directional second derivatives on real-space traces of quantified density contribution made by each orbital along the λ_2-eigenvector. The latter step is used to characterize each orbital as *concentrating*, *depleting*, or *noncontributing* to the total ED at the selected **r** when, respectively, second derivative is negative, positive, or an MO node is observed. Finally, orbitals' contributions of the same nature can be grouped at each **r** along the λ_2-eigenvector to generate traces of the total concentrating, depleting and noncontributing character. Relevant MO-ED data obtained for a planar equilibrium LiH dimer is shown in Figure 5. A molecular graph (see inset in Figure 5b) reveals four legitimate DB(Li,H) linking atoms involved in highly attractive −160.6 kcal/mol diatomic interaction. However, one can also see highly questionable[44] DB(H,H) between H-atoms involved in highly repulsive +86 kcal/mol interaction (with d(H,H) = 2.673 ≫ 2.4 Å; sum of van der Waals atomic radii) but no DB is observed between Li-atoms. Among 98 orbitals at the CCSD level, two bonding-antibonding MO-pairs (see Figure 5a) contain 98% of the total electron count; hence, they must shape the density distribution throughout this molecule such that features of a molecular graph (DBs, CPs, or their absence) can be fully recovered. To this effect:

1. Considering the CP(Li,H) and using an orthodox classification of orbitals, bonding (χ_3) and antibonding (χ_4) orbitals contribute nearly exactly the same 37%-fraction to the *tot*-ED - see Figure 5a. The core electrons are not expected to be involved in chemical bonding but σ_1-bonding χ_1 and σ^*_1-antibonding χ_2 orbitals contribute significantly to the *tot*-ED at CP(Li,H), 11.8% each. Importantly, all four orbitals *concentrate* ED at and in the vicinity of the CP(Li,H) and this is confirmed by negative directional partial second derivatives in Figure 5e. Clearly, this is contrary to classical thinking.
2. Only σ_2-bonding natural orbital (NO, χ_3) concentrates ED at CP(H,H)—see solid-line traces χ_3–H,H in Figures 5c,f. This single "bonding" contribution overwrites the other orbitals' contributions such that the directional partial second derivative computed for the *tot*-ED is negative in the vicinity of CP(H,H)—see the trace Total-H,H in Figure 5d. This shows that exactly the same orbital-determined features, that is, the dominant density contribution in concentrating fashion to the bonding internuclear Li,H and H,H regions takes place. Consequently, both atom-pairs are linked with a DB regardless of the attractive or repulsive nature of an interaction atoms are involved in.
3. The Li···Li interaction has no DB and this is recovered by MO-ED data. A marginal concentrating contribution to the *tot*-ED at the MDP(Li,Li) is made by χ_1 (see dashed-line χ_1-Li,Li traces in Figures 5b,f) but major and depleting ED contribution is made by the χ_3 orbital—see dashed-line χ_3-Li,Li traces in Figure 5c,f. Consequently, the partial directional second derivative computed for the *tot*-ED is positive at and the vicinity of the MDP(Li,Li)—see the Total-Li,Li trace-line in Figure 5d.

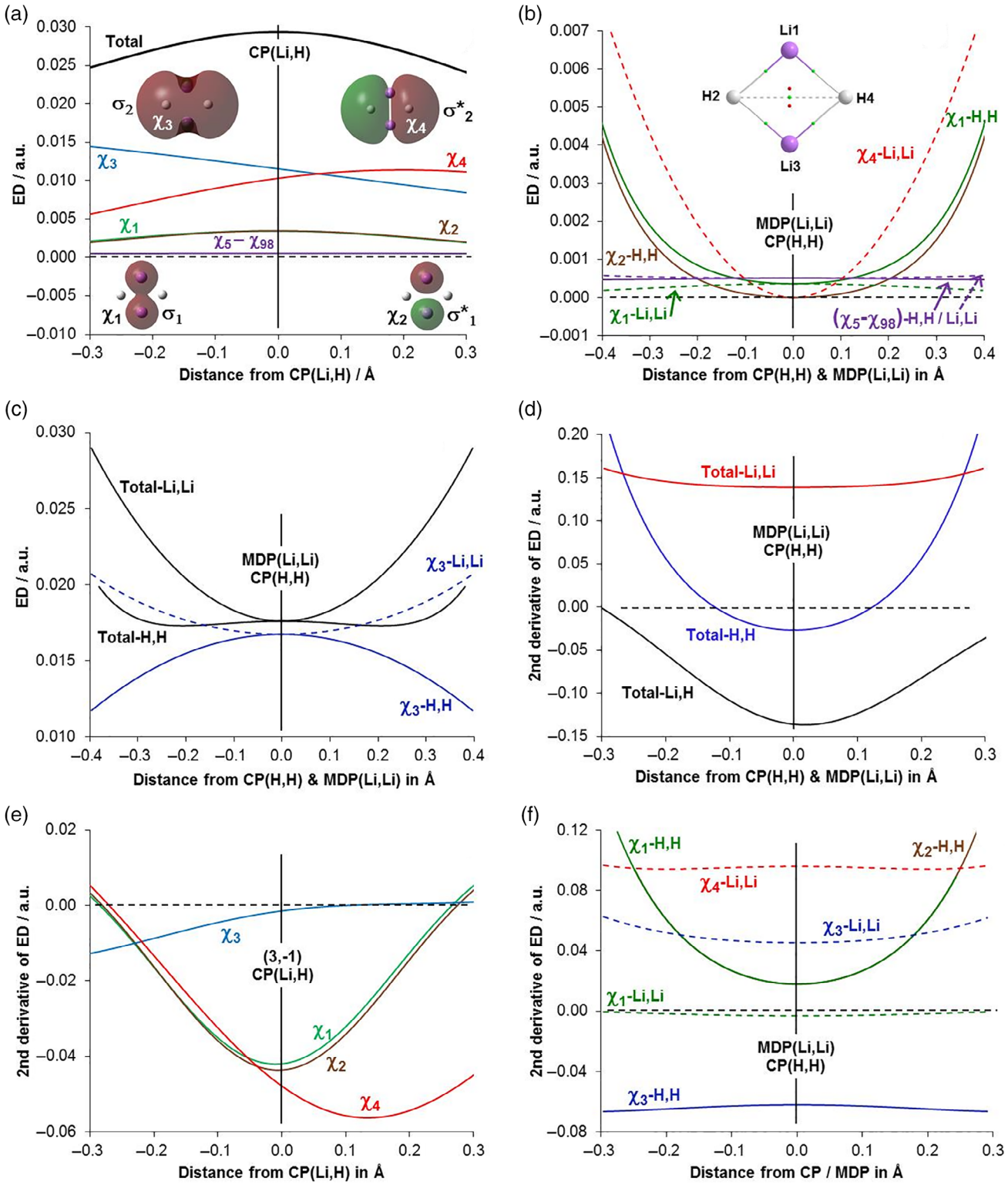

FIGURE 5 Trends obtained at the CCSD level from the MO-ED method, computed from a 1D cross-section along appropriate λ-eigenvectors, showing contributions made by the indicated individual highest occupied orbitals at and in the vicinity of: (a) CP(Li,H); (b and c) CP(H,H) and MDP(Li.Li) for small and significant ED contributions at CP/MDP, respectively, in LiH dimer. Directional partial second derivatives computed on the trends representing *tot*-ED are shown in part d and those obtained for individual orbitals are shown in part e (for DBs with CP(Li,H)) and in pat f (for DB with CP(H,H) and for MDP(Li,Li)). 3D-isosurfaces of the highest-occupied NOs and a molecular graph of LiH dimer are shown as insets in part a and b, respectively. Adapted from Reference 43

Finally, results in Figure 5 demonstrate that orbitals make throughout-a-molecule contributions of dramatically different nature, often in contradiction to the orthodox interpretations. To this effect: (i) the core 1s and classical σ_1-bonding NO (χ_1) concentrates ED at CP(Li,H) (11.8% of the *tot*-ED) but depletes at CP(H,H) and concentrates again at the MDP(Li,Li) by about 2% of the *tot*-ED whereas (ii) classical σ^*_1-antibonding NO (χ_2) also concentrates 11.8% at the CP(Li,H).

3.3.2 | Insight from the MO-DI method

The MO-DI protocol was developed[43] to decompose the diatomic electron delocalization into quantitative contributions made by individual and paired orbitals to the total QTAIM-defined delocalization index *DI*(A,B). To this effect, one defines an AOM for an atom A, which satisfies $N(\mathrm{A}) = tr(\mathrm{S^A})$, where N(A) is the total electronic population, and its elements are

$$S_{ij}^{\mathrm{A}} = \sum_{ij} \int_{\mathrm{A}} \sqrt{\nu_i}\sqrt{\nu_j}\chi_i^*(\mathbf{r})\chi_j(\mathbf{r})\mathrm{d}\mathbf{r} \tag{16}$$

Next, a delocalized density matrix for atom-pair A,B is defined with elements

$$D_{ij}^{(\mathrm{A,B})}| = 2\left|-S_{ij}^{\mathrm{A}}S_{ij}^{\mathrm{B}}\right| \tag{17}$$

These elements sum up to the orthodox QTAIM delocalization index *DI*(A,B). The resultant delocalized density matrix provides invaluable quantified data, namely:

a. Individual MO's contribution is recovered from diagonal elements.
b. The increasing (or decreasing) nature of paired orbitals, in terms of delocalized electron-pair contributions, through either constructive or deconstructive interference, is obtained from off-diagonal elements.
c. The interference-corrected net individual orbital's contribution is recovered by summing values in rows or columns.

As an example, data obtained for the H···H interaction in the LiH dimer[43] is presented in Table 1. Using an orthodox language applicable to chemical bonding:

1. The core 1s σ_1-bonding and σ^*_1-antibonding NOs do not participate in bonding as they do not delocalize electron-pairs (see first two columns in Table 1). They do, however, contribute a little (2%) to the *tot*-ED, but in a depleting fashion as seen in Figure 5b.
2. The "valence" σ_2-bonding (χ_3) and σ^*_2-antibonding (χ_4) NOs are indeed involved in chemical bonding between highly repulsive H-atoms in LiH dimer. These NOs delocalize close to a single pair of electrons each, 0.85 and 0.88 *e*-pairs at CP(H,H), respectively (see diagonal bold values, columns 3 and 4 in Table 1). However, due to deconstructive interference of −0.82 *e*-pairs between χ_3 and χ_4, their delocalization has been reduced to 0.04 and 0.06 *e*-pairs, respectively.

3.3.3 | Combining conclusions arrived at from MO-ED and MO-DI

Combining data from MO-ED and MO-DI approaches provides a lot of insight on properties of density in the "bonding" internuclear region. It is clear that the same underlying processes produced highly comparable $DI(\mathrm{Li,H}) = 0.12$ and $DI(\mathrm{H,H}) = 0.10$ as well as DB(Li,H) and DB(H,H) in the LiH dimer. This nicely explains and quantifies orbital's roles and inputs made to concentrating ED and delocalizing *e*-pairs in the internuclear region, that is, two fundamental and energy-lowering mechanisms of chemical bonding.

TABLE 1 Individual and paired NO's contributions to the total *DI*(A,B) obtained at the CCSD level from the MO-DI method for the H···H interaction in the LiH dimer

	H···H interaction				
NO	**1**	**2**	**3**	**4**	**5–98**
1	**0.00**	0.00	0.00	0.00	0.00
2	0.00	**0.00**	0.00	0.00	0.00
3	0.00	0.00	**0.85**	−0.82	0.00
4	0.00	0.00	−0.82	**0.88**	−0.01
5–98	0.00	0.00	0.00	−0.01	**0.00**
Sum	0.00	0.00	0.04	0.06	0.00
%-fraction	0	0	37	63	−1

The MO-ED and MO-DI methodologies revealed[35] that *exactly the same* physical processes that govern density accumulation and delocalization between H-atoms of a bay in the planar and twisted bph[35] take place at CPs and MDPs and their vicinity regardless of:

1. The nature of a diatomic interaction (either highly attractive or repulsive),
2. Presence or absence of a DB; the same Physics governs (a) classical C—C and C—H covalent bonds in the planar biphenyl (bph); (b) a DB-free H···H interaction in the LEC of bph, or (c) weakly interacting (in attractive fashion) and DB-linked H-atoms in the planar bph (seen by orthodox chemists as repulsive steric clash),
3. H-atoms involved in three highly repulsive (over +80 kcal/mol) interactions and each H,H-pair linked by a DB in cubic LiH.

Hence, if one accepts a DB-CP feature as representing a completed process of chemical bonding in the equilibrium structure, for example, the classical C–C and C–H single covalent bonds, then there is no obvious reason to reject a notion that all DBs on a molecular graph represent energy contributions of bonding nature.

Moreover, the presence of DB only in planar bph was perfectly explained by the use of the $CP(\mathbf{r})$ function.[45] This function accounts for the rate of change of facilitating (concentrating ED) relative to hindering (depleting ED) factors in the vicinity of either a CP or MDP. Importantly, the $CP(\mathbf{r})$ function can be used: (1) in any internuclear region, (2) at any level of theory, (3) for attractive and repulsive (non)bonded interactions, and (4) in (non)equilibrium structures.[46] It can be also applied equally well using combined concentrating and depleting contributions obtained either from MO-based[35] or FALDI-based[45] methods.

4 | FAMSEC-BASED METHODS IN EXPLORING THE MOLECULAR-WIDE AND DENSITY BASED CONCEPT OF CHEMICAL BONDING

A multi-centric,[37,45,47] multi-orbital,[35,43,47] and molecular-wide[46] nature of a "diatomic" interaction strongly questions not only an orthodox concept of a chemical 2-atom bond in a multi-nuclei environment but the *chemical bond* unicorn altogether. Many molecules or their fragments are highly "flexible" and, due to structural rearrangement, form numerous and comparable in stability 3D constellations of nuclei (conformers or isomers) with an intact major network of diatomic interactions (classical covalent bonds) but very different set of intramolecular interactions between classically nonbonded atoms. Even more complex are molecular systems made of two or more molecules, as they rearrange their structures and relative positions to each other in order to minimize the overall poly-molecular system energy. These structural rearrangements are driven by intra- and intermolecular interactions while keeping a molecular skeleton unchanged. To provide a qualitative and quantitative description of interactions driving a chemical change, the FAMSEC method[19] quantifies the impact made by the immediate and distant environment on (i) energies of molecular n-atom fragments, $1 \le n \le k$ (where k = number of atoms in a molecule), (ii) intra- and interfragment interaction energies, and (iii) fragments' energy contributions to molecular (in)stability. FAMSEC family of methods makes use of the IQA-defined[16,17] principle energy terms, that is, self-atomic and diatomic interaction energies. They are incorporated in

the FAMSEC-defined energy terms that, in turn, are designed to describe a specific chemical event by accounting for energy changes *throughout entire molecular system*. Hence, all atoms and interactions are treated on equal footing (in the FAMSEC world no chemical bonds exist) and "philosophy" adopted in FAMSEC proved to be useful in the study of:

1. Intramolecular interactions: classical NH···N (in protonated ethylenediamine) and NH···O (in protonated ethanolamine), highly repulsive O···O in eclipsed glycol, and controversial CH···HC interaction in planar biphenyl.[19] Their nature, strength, and impact on molecular stability was explained.
2. Relative stability of Be(II)[48] and Zn(II)[49] complexes with nitrilotriacetic acid and nitrilotri-3-propionic acid using Preorganized-Interacting Fragments Attributed Relative Molecular Stability (π-FARMS) method, a related version of FAMSEC.
3. Factors impacting stability of the 2-buthene conformers (*cis*-eq, *cis*-TS, *trans*-eq, and *trans*-TS) and rotational energy barrier of a methyl group.[50]

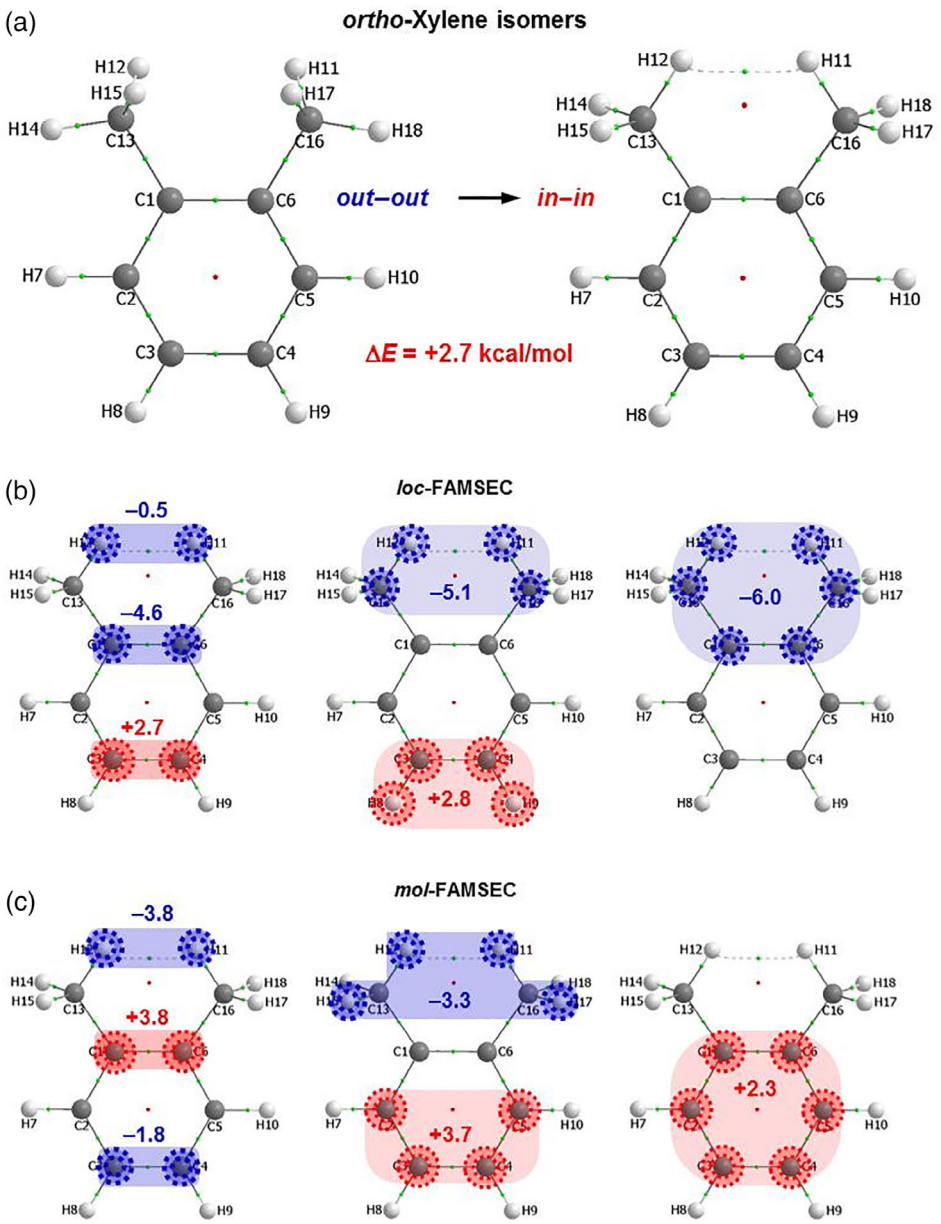

FIGURE 6 Molecular graphs of *out–out* and *in–in ortho*-xylene isomers— (a). Energy topologies of *loc*-FAMSEC (b) and *mol*-FAMSEC (c) were computed on the *out–out* → *in–in* structural change at the MP2/aug-cc-pVDZ level; all values in kcal/mol. Contributions of stabilizing and destabilizing nature are color-coded as blue and red, respectively. Adapted from Reference 60

4. Intramolecular red- (O—H···N) and blue-shifted (N—H···O) H-bonds involving the same heteroatoms in conformers of β-alanine.[42]
5. Relative stability of linear, staggered, and eclipsed conformers of glycol.[51,52]
6. Relative stability and affinity to acetone of S-proline conformers, the mechanism of the proline catalyzed aldol reaction,[53] and a nucleophilic substitution of 2-phenylquinoxaline[54] using a REP-FAMSEC (reaction energy profile-FAMSEC) protocol.[53]

FAMSEC and the arsenal of methods considered as modern chemical bonding and electronic structure descriptors (Electron Density of Delocalized Bonds,[55] Harmonic Oscillator Model of Aromaticity,[56] Nucleus-Independent Chemical Shifts,[57] FALDI, Extended Transition State–Natural Orbitals for Chemical Valence,[58] Domain-Averaged Fermi Holes,[59] QTAIM, and IQA) were used to investigate relative stability of *in–in* and *out–out* isomers of *ortho*-xylene.[60] Highly consistent multi-method results showed that focusing on H11,H12 atom-pair involved in steric contact or even immediate environment (the bay and two methane functional groups) in the *in–in* isomer cannot explain relative stability of the two molecules. Only by exploring the changes in the electronic structure of the entire molecule one can point at sources of these conformers' relative stability. An example of an insight gained from the FAMSEC-based analysis is shown in Figure 6; molecular fragments are marked in blue and red when they made energy contribution of a stabilizing and destabilizing nature, respectively. FAMSEC can provide a topology of *n*-atom fragments but only the most significant 2-, 4-, and 6-atom energy contributions (in kcal/mol) on the *out–out* → *in–in* transformation are shown for atoms linked by a continues network of DBs plus relevant fragments containing clashing H-atoms.

It is apparent (Figure 6b) that H12···H11, C13H12···H11C16, and entire bay became more stable (their energy decreased) on the *out–out* → *in–in* structural change as shown by *loc*-FAMSEC <0. Even more surprising, when classical interpretations are considered, the *in–in* isomer was stabilized the most by H12···H11 among 2-atom fragments with *mol*-FAMSEC = −3.8 kcal/mol and (H15)H12···H11(H17) with *mol*-FAMSEC = −3.3 kcal/mol among 4-atom fragments—Figure 6c. Actually, the H11 and H12 atoms became most stabilized and their IQA-defined additive energy decreased by −1.1 kcal/mol each when in *in–in*. Many fragments destabilize the *in–in* relative to *out–out* conformer and the ones that made largest contributions are found mainly at the bottom of the molecule or are part of benzene ring.

5 | CONCLUSIONS

Bader's molecular graph reveals a network of DBs linking two atoms in accord with overwhelming majority of well-localized classical chemical bonds, that is, two-center two-electron bonds (2c—2e). Whereas most of DBs are between atoms classically seen as chemically bonded in a specific molecular environment, they are also present where chemical bonds, according to an orthodox view, do not exist, for example, between atoms involved in a repulsive interaction. Many, or maybe most chemists, also disagree with Bader's notion that a DB represents chemical bonding (not necessarily a chemical bond). However, it has been proved that MOs support energy-stabilizing "bonding" nature of Bader's BP that "pin-points universal physical and net energy-lowering processes that might, but do not have to, lead to a chemical bond formation."[35] Moreover, physical processes leading to the formation of a DB and a dominant constructive overlap of orbitals found for most common covalent bonds also occur between atoms involved in highly repulsive interactions.[35,43] Clearly, the density topology and processes leading to density distribution among atoms of a molecular system know nothing about chemical bonds.

Uncovering details of nonuniform density distribution is the domain of the NCI-plot method. It also fully recovers a network of CPs found from a molecular graph; hence, it carries the same ambiguity and uncertainty as QTAIM when interpretation of DB/CP feature in terms of chemical bonding goes. In principle, the nonuniform density distribution might be linked with a multi-center interaction (bonding) but, unfortunately, the NCI-plot method cannot pinpoint either (1) the origin of local ED depletion or accumulation; hence, no supported explanation in terms of chemical bonding can be provided, or (2) energetic contribution made by these departures from density uniformity.

Although not exclusively, the concept of multicenter bonds is often linked with another property that is not an observable, namely aromaticity unicorn. Interestingly, the MO multicenter bond index $I_{ABC...L}$, (it was initially developed to quantify the three-center character of intramolecular bonds in simple inorganic molecules and intermolecular hydrogen bonds involving peptides[61]) was used to measure aromaticity in different rings in a number of polycyclic

compounds.[62] Numerous concepts of multicenter bonds and related indexes were reported[55,56,63,64] showing that classical 2c—2e bonds fail to explain many known bonding modes.

In this contribution a concept of all-atom molecular-wide "bonding" is strongly advocated and protocols designed to investigate and quantify density concentration and delocalization (two physical processes that are synonymous with the concept of *chemical bonding*) at any coordinate **r** within a molecular system are described.

Using 1D cross sections along the λ_2-eigenvector originating from a CP on a DB linking two atoms involved in the intermolecular classical (i) H-bond between two water molecules and (ii) repulsive interaction between O-atoms of two water molecules were found to be qualitatively exactly the same, essentially indistinguishable. It became clear that DBs linking all *intermolecular* attractive and repulsive interactions have *the same density profile even though one computes different sets of topological properties at respective CPs* and this must reflect an impact made by a molecular environment.

FALDI performs density analysis over the entire molecular space in order to quantify localized and delocalized by all atoms ED at any coordinate **r**; hence, one can also combine FALDI with the 1D cross section methodology to explore the origin and composition of density at any CP. The qualitative FALDI-based data showed a multi-centric and molecular-wide character of a DB at a CP and its close vicinity; it pinpointed atoms and atom-pairs that contributed to the total ED and quantified each contribution. The same qualitative and quantitative FALDI-based analysis can be performed between atoms without a DB and this conclusively showed that: (1) molecular energy minimizing physical processes leading to concentration ED in and delocalization of ED into internuclear region do take place regardless of a presence or absence of a DB and (2) the presence of a DB simply signifies that the rate of concentrating ED at a coordinate **r** is larger than depleting of ED. Consequently, a universal $CP(\mathbf{r})$ function was proposed that explains presence or absence of a DB.

Partitioning the total ED to individual molecular or natural orbital's contributions, in conjunction with 1D cross section methodology, provides an orbital-based molecular-wide picture. The MO-ED and MO-DI methods, besides reproducing results from FALDI, provide qualitative description of orbitals' nature (it correlates well with classical understanding of bonding, nonbonding and antibonding orbitals) and quantitative contributions to the total ED made at any coordinate **r** by individual MOs.

Since the above protocols are valid at any coordinate **r**, they must also be applicable at the NCI-identified coordinates, where nonuniform density distribution occurs. Hence, in principle, the origin of processes leading to the nonuniform accumulation or depletion of ED can be identified and individual atomic or molecular fragment's contributions quantified.

The FAMSEC family of methods quantifies an impact of an immediate or distant molecular environment on intra- and intermolecular di-atomic, intra- and interfragment interactions and this includes classical chemical bonds and nonbonded interactions. This is achieved without an artificial partitioning of a molecule; a suitable reference molecular structure is used instead. Relative to the reference state, a computed change in atoms, molecular fragments (entire molecules) energy as well as strength and nature of interactions provides an invaluable insight on for example, relative stability of conformers and metal complexes (using a π-FARMS method), or a chemical change by explaining reaction mechanisms using the REP-FAMSEC approach.

The approaches described here (FALDI, FAMSEC, MO-ED, MO-DI, etc.), by making use of uniform, consistent and quantifiable physical processes provide a harmonious description of *molecular-wide and all-atoms chemical bonding* that either keeps a chemical identity intact (i.e., molecules and molecular assemblies) or drives a chemical change. In each case, the resultant (equilibrium) or in transition (e.g., at a transition state) density topology and physical processes leading to minimizing molecular system energy can be explained. Molecular fragments driving a chemical change can be identified and used to explain molecular system stability and chemical reactivity. One hopes that methodologies described constitute just a nucleus of complementing each other and operating in unison methods describing and explaining chemical processes using universal laws rather than unnecessary unicorns.

CONFLICT OF INTEREST

The author has declared no conflicts of interest for this article.

DATA AVAILABILITY STATEMENT

Data sharing is not applicable to this article as no new data were created or analyzed in this study.

ORCID

Ignacy Cukrowski https://orcid.org/0000-0001-8007-5675

RELATED WIREs ARTICLES

NCIPLOT and the analysis of noncovalent interactions using the reduced density gradient

Toward computational design of chemical reactions with reaction phase diagram

REFERENCES

1. Frenking G, Shaik S, editors. The chemical bond: fundamental aspects of chemical bonding. Weinheim, Germany: Wiley-VCH Verlag GmbH, & Co, KGaA; 2014.
2. Frenking G, Shaik S, editors. The chemical bond: chemical bonding across the periodic table. Weinheim, Germany: Wiley-VCH Verlag GmbH & Co, KGaA; 2014.
3. Grabowski SJ. Understanding hydrogen bonds: theoretical and experimental views. London, UK: RSC; 2020.
4. Grabowski SJ, editor. Hydrogen bonding—New insights. Dordrecht, The Netherlands: Springer; 2006.
5. Bakhmutov VI. Dihydrogen bonds. Principles, experiments, and applications. Hoboken, NJ: John Wiley & Sons, Inc; 2008.
6. Weinhold F, Landis CR. Valency and bonding. A natural bond orbital donor–acceptor perspective. Cambridge, UK: Cambridge University Press; 2005.
7. Gillespie RJ, Popelier PLA. Chemical bonding and molecular geometry. From Lewis to electron density, Oxford, UK: Oxford University Press; 2001.
8. Franking G, Krapp A. Unicorns in the world of chemical bonding models. J Comput Chem. 2007;28:15–24.
9. Hirshfeld FL. Bonded-atom fragments for describing molecular charge densities. Theoret Chim Acta (Berl). 1977;44:129–38.
10. Mayer I. Bond order and valence indices: a personal account. J Comput Chem. 2007;28:204–21.
11. Bader RFW. Atoms in molecules: a quantum theory. Oxford: Oxford University Press; 1990.
12. Flaig R, Koritsanszky T, Dittrich B, Wagner A, Luger P. Intra- and intermolecular topological properties of amino acids: a comparative study of experimental and theoretical results. J Am Chem Soc. 2002;124:3407–17.
13. Wolstenholme DJ, Matta CF, Cameron TS. Experimental and theoretical electron density study of a highly twisted polycyclic aromatic hydrocarbon: 4-methyl-[4]helicene. J Phys Chem A. 2007;111:8803–13.
14. Bader RFW. Bond paths are not chemical bonds. J Phys Chem A. 2009;113:10391–6.
15. Matta CF, Hernández-Trujillo J, Tang T-H, Bader RFW. Hydrogen–hydrogen bonding: a stabilizing interaction in molecules and crystals. Chem A Eur J. 2003;9:1940–51.
16. Blanco MA, Pendás AM, Francisco E. Interacting quantum atoms: a correlated energy decomposition scheme based on the quantum theory of atoms in molecules. J Chem Theory Comput. 2005;1:1096–109.
17. Francisco E, Pendás AM, Blanco MA. A molecular energy decomposition scheme for atoms in molecules. J Chem Theory Comput. 2006;2:90–102.
18. Geldof D, Krishtal A, Blockhuys F, Van Alsenoy C. An extension of the Hirshfeld method to open shell systems using fractional occupations. J Chem Theory Comput. 2011;7:1328–35.
19. Cukrowski I. IQA-embedded fragment attributed molecular system energy change in exploring intramolecular interactions. Comput Theoret Chem. 2015;1066:62–75.
20. Grimme S, Mück-Lichtenfeld C, Erker G, Kehr G, Wang H, Beckers H, et al. When do interacting atoms form a chemical bond? Spectroscopic measurements and theoretical analyses of dideuteriophenanthrene. Angew Chem Int Ed. 2009;48:2592–5.
21. Hancock RD, Nikolayenko IV. Do nonbonded H—H interactions in phenanthrene stabilize it relative to anthracene? A possible resolution to this question and its implications for ligands such as 2,2′-bipyridyl. J Phys Chem A. 2012;116:8572–83.
22. Adeyinka AS, Cukrowski I. Structural-topological preferences and protonation sequence of aliphatic polyamines: a theoretical case study of tetramine *trien*. J Mol Model. 2015;21:162.
23. Pendás AM, Francisco E, Blanco MA, Gatti C. Bond paths as privileged exchange channels. Chem A Eur J. 2007;13:9362–71.
24. Arunan E, Desiraju GR, Klein RA, Sadlej J, Scheiner S, Alkorta I, et al. Defining the hydrogen bond: an account (IUPAC technical report). Pure Appl Chem. 2011;83:1619–36.
25. Arunan E, Desiraju GR, Klein RA, Sadlej J, Scheiner S, Alkorta I, et al. Definition of the hydrogen bond (IUPAC recommendations 2011). Pure Appl Chem. 2011;83:1637–41.
26. Poater J, Sol M, Bickelhaupt FM. Hydrogen–hydrogen bonding in planar biphenyl, predicted by atoms-in-molecules theory, does not exist. Chem A Eur J. 2006;12:2889–95.
27. Bickelhaupt FM, Baerends EJ. The case for steric repulsion causing the staggered conformation of ethane. Angew Chem Int Ed. 2003;42:4183–8.
28. Bader RFW. Pauli repulsions exist only in the eye of the beholder. Chem A Eur J. 2006;12:2896–901.
29. Foroutan-Nejad C, Shahbazian S, Marek R. Toward a consistent interpretation of the QTAIM: tortuous link between chemical bonds, interactions, and bond/line paths. Chem A Eur J. 2014;20:10140–52.
30. Shahbazian S. Why bond critical points are not "bond" critical points. Chem A Eur J. 2018;24:5401–5.

31. Cukrowski I, de Lange JH, Adeyinka AS, Mangondo P. Evaluating common QTAIM and NCI interpretations of the electron density concentration through IQA interaction energies and 1D cross-sections of the electron and deformation density distributions. Comp Theoret Chem. 2015;1053:60–76.
32. Johnson ER, Keinan S, Mori-Sánchez P, Contreras-García J, Cohen AJ, Yang WJ. Revealing noncovalent interactions. J Am Chem Soc. 2010;132:6498–506.
33. Gillet N, Chaudret R, Contreras-García J, Yang W, Silvi B, Piquemal JP. Coupling quantum interpretative techniques: another look at chemical mechanisms in organic reactions. Chem Theory Comput. 2012;8:3993–7.
34. Contreras-García J, Johnson ER, Keinan S, Chaudret R, Piquemal JP, Beratan D, et al. NCIPLOT: a program for plotting noncovalent interaction regions. Chem Theory Comput. 2011;7:625–32.
35. Cukrowski I, de Lange JH, van Niekerk DM, Bates TG. Molecular orbitals support energy-stabilizing "bonding" nature of Bader's bond paths. J Phys Chem A. 2020;124:5523–33.
36. de Lange JH, Cukrowski I. Towards deformation densities for intramolecular interactions without radical reference states using the fragment, atom, localized, delocalized and interatomic (FALDI) charge density decomposition scheme. J Comput Chem. 2017;38:981–97.
37. de Lange JH, van Niekerk DM, Cukrowski I. FALDI-based decomposition of an atomic interaction line leads to 3D representation of the multicentre nature of interactions. J Comput Chem. 2018;39:973–85.
38. de Lange JH, Cukrowski I. Exact and exclusive electron localization indices within QTAIM atomic basins. J Comput Chem. 2018;39:1517–30.
39. Ponec R. Electron pairing and chemical bonds. Chemical structure, valences and structural similarities from the analysis of the Fermi holes. J Math Chem. 1997;21:323–33.
40. Ponec R. Electron pairing and chemical bonds. Molecular structure from the analysis of pair densities and related quantities. J Math Chem. 1998;23:85–103.
41. Ponec R, Duben AJ. Electron pairing and chemical bonds: bonding in hypervalent molecules from analysis of Fermi holes. J Comput Chem. 1999;20:760–71.
42. Cukrowski I, van Niekerk DM, de Lange JH. Exploring fundamental differences between red- and blue-shifted intramolecular hydrogen bonds using FAMSEC, FALDI, IQA and QTAIM. Struct Chem. 2017;28:1429–44.
43. de Lange JH, van Niekerk DM, Cukrowski I. Quantifying individual (anti)bonding molecular orbitals' contributions to chemical bonding. Phys Chem Chem Phys. 2019;21:20988–98.
44. Dem'yanov P, Polestshuk P. A bond path and an attractive Ehrenfest force do not necessarily indicate bonding interactions: case study on M_2X_2 (M=li, Na, K; X=H, OH, F, cl). Chem A Eur J. 2012;18:4982–93.
45. de Lange JH, van Niekerk DM, Cukrowski I. FALDI-based criterion for and the origin of an electron density bridge with an associated (3,–1) critical point on Bader's molecular graph. J Comput Chem. 2018;39:2283–99.
46. Bates TG, de Lange JH, Cukrowski I. The CH···HC interaction in biphenyl is a delocalized, molecular-wide and entirely non-classical interaction: results from FALDI analysis. J Comput Chem. 2021;42:706–18.
47. de Beer S, Cukrowski I, de Lange JH. Characterization of bonding modes in metal complexes through electron density cross-sections. J Comput Chem. 2020;41:2695–706.
48. Cukrowski I, Mangondo P. Interacting quantum fragments-rooted preorganized-interacting fragments attributed relative molecular stability of the Be^{II} complexes of nitrilotriacetic acid and nitrilotri-3-propionic acid. J Comput Chem. 2016;37:1373–87.
49. Mangondo P, Cukrowski I. On the origin of the relative stability of Zn^{II}NTA and Zn^{II}NTPA metal complexes. An insight from the IQA, IQF, and π-FARMS methods. Int J Quantum Chem. 2017;117:e25321.
50. Cukrowski I, Sagan F, Mitoraj MP. On the stability of *cis*- and *trans*-2-butene isomers. An insight based on the FAMSEC, IQA, and ETS-NOCV schemes. J Comput Chem. 2016;37:2783–98.
51. Cukrowski I, Polestshuk PM. Reliability of interacting quantum atoms (IQA) data computed from post-HF densities: impact of approximation used. Phys Chem Chem Phys. 2017;19:16375–86.
52. Cukrowski I. Reliability of HF/IQA, B3LYP/IQA, and MP2/IQA data in interpreting the nature and strength of interactions. Phys Chem Chem Phys. 2019;21:10244–60.
53. Cukrowski I, Dhimba G, Riley DL. Reaction energy profile and fragment attributed molecular system energy change (FAMSEC)-based protocol designed to uncover reaction mechanism: a case study of the proline catalyzed aldol reaction. Phys Chem Chem Phys. 2019;21:16694–705.
54. Mdhluli KB, Nxumalo W, Cukrowski I. A REP-FAMSEC method as a tool in explaining reaction mechanisms: a nucleophilic substitution of 2-phenylquinoxaline as a DFT case study. Molecules. 2021;26:1570.
55. Szczepanik DW, Andrzejak M, Dyduch K, Żak E, Makowski M, Mazur G, et al. A uniform approach to the description of multicenter bonding. Phys Chem Chem Phys. 2014;16:20514–23.
56. Kruszewski J, Krygowski TM. Definition of aromaticity basing on the harmonic oscillator model. Tetrahedron Let. 1972;13:3839–42.
57. Schleyer PR, Maerker C, Dransfeld A, Jiao H, NJRvE H. Nucleus-independent chemical shifts: a simple and efficient Aromaticity probe. J Am Chem Soc. 1996;118:6317–8.
58. Mitoraj MP, Michalak A, Ziegler T. A combined charge and energy decomposition scheme for bond analysis. J Chem Theory Comput. 2009;5:962–75.
59. Ponec R, Roithová J. Domain-averaged Fermi holes – a new means of visualization of chemical bonds. Bonding in hypervalent molecules. Theoret Chem Acc. 2001;105:383–92.

60. Mitoraj MP, Sagan F, Szczepanik DW, de Lange JH, Ptaszek AL, van Niekerk DM, et al. Origin of hydrocarbons stability from computational perspective – a case study of xylene isomers. ChemPhysChem. 2020;21:494–502.
61. Giambiagi M, de Giarnbiagi MS, Mundimt KC. Definition of a multicenter bond index. Struct Chem. 1990;1:423–7.
62. Giambiagi M, de Giambiagi MS, dos Santos Silva CD, de Figueiredo AP. Multicenter bond indices as a measure of aromaticity. Phys Chem Chem Phys. 2000;2:3381–92.
63. Bultinck P, Ponec R, van Damme S. Multicenter bond indices as a new measure of aromaticity in polycyclic aromatic hydrocarbons. J Phys Org Chem. 2005;18:706–18.
64. Bultinck P, Rafat M, Ponec R, van Gheluwe B, Carbó-Dorca R, Popelier P. Electron delocalization and aromaticity in linear polyacenes: atoms in molecules multicenter delocalization index. J Phys Chem A. 2006;110:7642–8.

How to cite this article: Cukrowski I. A unified molecular-wide and electron density based concept of chemical bonding. WIREs Comput Mol Sci. 2022;12:e1579. https://doi.org/10.1002/wcms.1579